ORIGINAL ARTICLE

Undifferenced ionospheric-free ambiguity resolution using GLONASS data from inhomogeneous stations

Qile Zhao[1] · Xiaotao Li[1] · Yang Liu[1] · Jianghui Geng[1,2] · Jingnan Liu[1]

Abstract

GLONASS frequency division multiple access signals render ambiguity resolution (AR) rather difficult because: (1) Different wavelengths are used by different satellites, and (2) pseudorange inter-frequency biases (IFBs) cannot be precisely modeled by means of a simple function. In this study, an AR approach based on the ionospheric-free combination with a wavelength of about 5.3 cm is assessed for GLONASS precise point positioning (PPP). This approach simplifies GLONASS AR because pseudorange IFBs do not matter, and PPP-AR can be enabled across inhomogeneous receivers. One month of GLONASS data from 165 European stations were processed for different network size and different durations of observation periods. We find that 89.9% of the fractional parts of ionospheric-free ambiguities agree well within ± 0.15 cycles for a small network (radius = 500 km), while 77.6% for a large network (radius = 2000 km). In case of the 3-hourly GLONASS-only static PPP solutions for the small network, reliable AR can be achieved where the number of fixed GLONASS ambiguities account for 97.6% within all candidate ambiguities. Meanwhile, the RMS of the east, north and up components with respect to daily solutions is improved from 1.0, 0.6, 1.2 cm to 0.4, 0.4, 1.1 cm, respectively. When GPS PPP-AR is carried out simultaneously, the positioning performance can be improved significantly such that the GLONASS ambiguity fixing rate rises from 74.4 to 95.4% in case of hourly solutions. Finally, we introduce ambiguity-fixed GLONASS orbits to re-attempt GLONASS PPP-AR in contrast to the above solutions with ambiguity-float orbits. We find that ambiguity-fixed orbits lead to clearly better agreement among ionospheric-free ambiguity fractional parts in case of the large network, that is 80.5% of fractional parts fall in ± 0.15 cycles in contrast to 74.6% for the ambiguity-float orbits. We conclude that highly efficient GLONASS ionospheric-free PPP-AR is achievable in case of a few hours of data when GPS PPP-AR is also accomplished, and ambiguity-fixed GLONASS orbits will contribute significantly to PPP-AR over wide areas.

Keywords Precise point positioning · GLONASS · Ionospheric-free ambiguity resolution · Fractional-cycle bias · Inhomogeneous stations

Introduction

In recent years, ambiguity resolution for precise pointing positioning (PPP-AR) has been of much interest since higher accuracy and faster initializations can be achieved in contrast to conventional float solutions (Bertiger et al. 2010; Collins et al. 2010; Laurichesse et al. 2009). Particularly, Ge et al. (2008) developed a GPS PPP-AR approach where the fractional-cycle biases (FCBs) of uncalibrated phase delays (UPDs) are produced across a reference network and then delivered to PPP users to enable AR at a single station. While this approach applies to all GNSS emitting code division multiple access (CDMA) signals, it does not apply to the GLONASS constellation, which transmits frequency division multiple access (FDMA) signals at the moment.

One important reason is that inter-frequency biases (IFBs) are present within both GLONASS pseudorange and carrier phase observations, which have to be corrected before attempting GLONASS AR (Leick et al. 1995; Sleewaegen et al. 2012; Wang 2000; Wang et al. 2001). Carrier phase IFBs are relatively stable over time and are usually presumed to precisely follow a linear function of the frequency channel number (Al-Shaery et al. 2013; Geng et al. 2017; Wanninger

✉ Jianghui Geng
jgeng@whu.edu.cn

[1] GNSS Research Center, Wuhan University, Wuhan, China

[2] Collaborative Innovation Center of Geospatial Technology, Wuhan, China

2012). However, such linear function normally breaks down for pseudorange IFBs. It has been reported that pseudorange IFBs vary with receivers, antennas, domes and firmware and hence, cannot be modeled using a simple function but should be addressed for individual stations and satellites (Reussner and Wanninger 2011; Shi et al. 2013; Yamada et al. 2010). It is the pseudorange IFBs that complicate GLONASS AR that relies on the Hatch–Melbourne–Wübbena combination observable (Hatch 1982) for long baseline positioning or PPP across inhomogeneous stations.

At present, two approaches have been developed to avoid or diminish the adverse impact of pseudorange IFBs on GLONASS PPP-AR for inhomogeneous stations. One idea is that predetermined ionospheric products, e.g., global ionospheric maps, can be introduced into the wide-lane carrier phase combination observable to compute its ambiguity, rather than by means of the Hatch–Melbourne–Wübbena combination (Reussner and Wanninger 2011). Based on raw observables, Geng and Bock (2016) directly constrained the line of sight ionospheric parameters with external ionospheric products and presented the full schemes to accomplish GLONASS PPP-AR across inhomogeneous stations, with the extra benefit of speeding up PPP convergence to ambiguity-fixed solutions (Geng and Shi 2017). However, the performance of this strategy is subject to the accuracy of ionospheric products, and a regional ionospheric product is preferred (Geng and Shi 2017). On the other hand, Banville (2016) proposed to fix ionospheric-free ambiguities with a wavelength of about 5.3 cm for GLONASS AR. Different from GPS ionospheric-free ambiguities, the GLONASS counterparts are integers in nature thanks to the ratio of 9/7 between the L1 and L2 frequencies. Banville (2016) calculated undifferenced ambiguities using PPP and formulated double-difference ambiguities over 12 baselines spanning 300–1400 km for integer cycle resolution. It is reported that ionospheric-free AR is indeed achievable, though shorter periods of data, e.g., 1 h, cannot efficiently guarantee a high fixing rate. Liu et al. (2016) showed that GLONASS ionospheric-free AR over baselines of longer than 2000 km using daily data could be accomplished with a fixing rate of over 80% and the agreement of orbit overlaps can be improved by more than 20%.

This study is dedicated to GLONASS PPP-AR over inhomogeneous stations where we exploit the performance of resolving undifferenced ionospheric-free ambiguities, which are both immune to pseudorange IFBs and exemption of first-order ionospheric delays. The only disadvantage of ionospheric-free ambiguities is their ultrashort wavelength of about 5.3 cm, which is exactly half of the narrow-lane wavelength. The ensuing question is what performance we can achieve when fixing them, especially in case of short durations of data, e.g., a few hours and networks of various scales, e.g., hundreds to thousands of kilometers, and in combination

with GPS PPP-AR. More interestingly, we will also investigate how the GLONASS orbits produced by fixing ionospheric-free ambiguities according to Liu et al. (2016) benefit GLONASS PPP-AR. We first present the mathematical model and the details of the ionospheric-free PPP-AR, then, describe the experiments and analyze the performance, and finally draw the conclusions.

Methods

In this section, we first give a brief introduction about GLONASS ionospheric-free observable. In addition, based on the idea of fixing ionospheric-free ambiguities with a wavelength of about 5.3 cm for GLONASS proposed by Banville (2016) and Liu et al. (2016), the details of GLONASS ionospheric-free FCBs estimation are presented. The receiver carrier phase IFBs of GLONASS must be calibrated before the FCB estimation.

GLONASS ionospheric-free observable

Undifferenced GLONASS observation equations of dual-frequency carrier phase and pseudorange measurements on frequency band ($g = 1, 2$) from receiver a to satellite i can be written as

$$
\begin{aligned}
P_{g,a}^i &= \rho_a^i + I_a^i/f_{g,k}^2 + B_{g,a}^i - B_g^i, \quad \varepsilon_{P_{g,a}^i} = \sigma_P \\
L_{g,a}^i &= \rho_a^i - I_a^i/f_{g,k}^2 + b_{g,a}^i - b_g^i + \lambda_g^k N_{g,a}^i, \quad \varepsilon_{L_{g,a}^i} = \sigma_L
\end{aligned}
\tag{1}
$$

where $P_{g,a}^i$ and $L_{g,a}^i$ are pseudorange and carrier phase measurements in the unit of length, with precisions of σ_P and σ_L, respectively; ρ_a^i denotes the non-dispersive delay including the geometric distance, the tropospheric and relativistic effects; k is the frequency channel number of satellite i; $f_{g,k}$ is the frequency of channel k on frequency band g ($g = 1, 2$); $I_a^i/f_{g,k}^2$ is the first-order ionospheric delay for $f_{g,k}$ $B_{g,a}^i$ and $b_{g,a}^i$ are uncalibrated pseudorange and carrier phase biases at station a, respectively. Correspondingly, B_g^i and b_g^i are pseudorange and carrier phase biases at satellite i, respectively; $N_{g,a}^i$ is the integer carrier phase ambiguity and is scaled by wavelength λ_g^k. Unmodeled errors such as multipath and higher order ionospheric effects are ignored for brevity.

For PPP, the ionospheric-free combination observable is usually used, that is

$$
\begin{aligned}
P_{if,a}^i &= \alpha P_{1,a}^i + \beta P_{2,a}^i = \rho_a^i + B_{if,a}^i - B_{if}^i \\
L_{if,a}^i &= \alpha L_{1,a}^i + \beta L_{2,a}^i = \rho_a^i + \alpha \lambda_1^k N_{1,a}^i + \beta \lambda_2^k N_{2,a}^i + b_{if,a}^i - b_{if}^i
\end{aligned}
\tag{2}
$$

where

$$B_{if,a}^i = \alpha B_{1,a}^i + \beta B_{2,a}^i$$
$$B_{if}^i = \alpha B_1^i + \beta B_2^i$$
$$b_{if,a}^i = \alpha b_{1,a}^i + \beta b_{2,a}^i$$
$$b_{if}^i = \alpha b_1^i + \beta b_2^i$$

and

$$\alpha = f_{1,k}^2 / \left(f_{1,k}^2 - f_{2,k}^2 \right)$$
$$\beta = -f_{2,k}^2 / \left(f_{1,k}^2 - f_{2,k}^2 \right)$$

The terms $B_{if,a}^i$, B_{if}^i, $b_{if,a}^i$ and b_{if}^i cannot be directly estimated, which are, however, absorbed into either observation residuals or other parameters such as clocks and ambiguities (Geng et al. 2010a). For example, $b_{if,a}^i$ and b_{if}^i will be combined with the ambiguity parameters, such that

$$\begin{aligned} \lambda_{if}^k N_{if,a}^i &= \alpha \lambda_1^k N_{1,a}^i + \beta \lambda_1^k N_{2,a}^i + b_{if,a}^i - b_{if}^i \\ &= \frac{9}{32} \lambda_1^k \left(9N_{1,a}^i - 7N_{2,a}^i \right) + b_{if,a}^i - b_{if}^i \\ &= \frac{1}{2} \lambda_n^k \left(9N_{1,a}^i - 7N_{2,a}^i \right) + b_{if,a}^i - b_{if}^i \end{aligned} \tag{3}$$

where λ_{if}^k and $N_{if,a}^i$ are the ionospheric-free wavelength and ambiguity, respectively; λ_n^k is narrow-lane wavelength. Defining

$$N_{N,a}^i = 9N_{1,a}^i - 7N_{2,a}^i$$

equation (3) can then be rewritten as

$$\lambda_{if}^k N_{if,a}^i = \lambda_{if}^k N_{N,a}^i + b_{if,a}^i - b_{if}^i \tag{4}$$

$N_{N,a}^i$ has integer nature and its wavelength, $\lambda_{if}^k = \frac{1}{2}\lambda_n^k$, is about 5.3 cm, which is exactly half of the narrow-lane wavelength (Dai 2000; Roßbach 2000).

GLONASS ionospheric-free FCB estimation

In the case of GPS data, single-difference ambiguities between satellite i and j are usually formed to eliminate the receiver dependent biases. However, considering that the wavelengths of GLONASS carrier phase data are not identical across different channels, and that carrier phase IFBs have a linear relationship with the channel number, we can obtain

$$\lambda_{if}^k N_{if,a}^i - \lambda_{if}^l N_{if,a}^j = \Delta\lambda_{if}^{kl} N_{N,a}^i + \lambda_{if}^l \Delta N_{N,a}^{ij} + \tau \cdot \Delta b_{if,a} - \Delta b_{if}^{ij} \tag{5}$$

where the channel number of satellite i and j is k and l, respectively, and $\tau = k - l$; $\Delta b_{if,a}$ is the ionospheric-free IFBs defined between adjacent channel number; and

$$\Delta N_{N,a}^{ij} = N_{N,a}^i - N_{N,a}^j$$
$$\Delta\lambda_{if}^{kl} = \lambda_{if}^k - \lambda_{if}^l, \ \left| \Delta\lambda_{if}^{kl} \right| \leq 0.245 \text{ mm}$$
$$\Delta b_{if}^{ij} = b_{if}^i - b_{if}^j$$

Note that $N_{N,a}^i$ and $\Delta N_{N,a}^{ij}$ cannot be estimated simultaneously due to rank deficiency. However, $N_{N,a}^i$ can be approximated using its corresponding ionospheric-free ambiguity estimate $N_{if,a}^i$. Since the wavelength of $N_{N,a}^i$ is as small as 0.245 mm, the discrepancy between the true values of $N_{if,a}^i$ and $N_{N,a}^i$ will negligibly bias $\Delta N_{N,a}^{ij}$. Moreover, $\Delta b_{if,a}$ can be calibrated using predetermined carrier phase IFBs (Wanninger 2012; Geng et al. 2017). Assuming that $\Delta b_{if,a}$ and $N_{N,a}^i$ are known, we move them to the left side of (5) and obtain

$$l_{if,a}^{kl} \Big/ \lambda_{if}^l = \Delta N_{N,a}^{ij} - \Delta b_{if}^{ij} \Big/ \lambda_{if}^l \tag{6}$$

where

$$l_{if,a}^{kl} = \lambda_{if}^k N_{if,a}^i - \lambda_{if}^l N_{if,a}^j - \Delta\lambda_{if}^{kl} N_{N,a}^i - \tau \cdot \Delta b_{if,a}$$

Equation (6) is the basis for the estimation of GLONASS ionospheric-free FCBs, and the fractional parts of a satellite pair can be obtained.

Once we obtain the fractional parts of all relevant $l_{if,a}^{kl} / \lambda_{if}^l$ for a satellite pair i and j using a reference network, we then average them to estimate single-difference FCBs (Ge et al. 2008; Cheng et al. 2017). Afterward, we select one satellite as the reference to convert all single-difference FCBs into undifferenced (pseudoabsolute) FCBs for PPP-AR. We note that rigorous FCB estimation should be achieved by first fixing double-difference ambiguities of the reference network, which, however, is not implemented in this study for convenience (Geng et al. 2012).

Data processing

We processed about 165 European stations from the EUREF (Europe Reference Frame) permanent network and IGS network, tracking both GPS and GLONASS, for the day of year (DOY) 300–330 in 2013 (Fig. 1). The number of receiver families involved in the network is seven (Table 1). Again, we stress that ionospheric-free PPP-AR can be straightforwardly applied to GLONASS stations with diverse receiver types, antennas, domes and firmware. European Space Agency (ESA) final GPS/GLONASS orbits, 30-s satellite clock corrections and earth rotation parameters were used. A 7° cutoff angle was set for usable observations, but 10° for eligible ambiguities used for FCB estimation and ambiguity
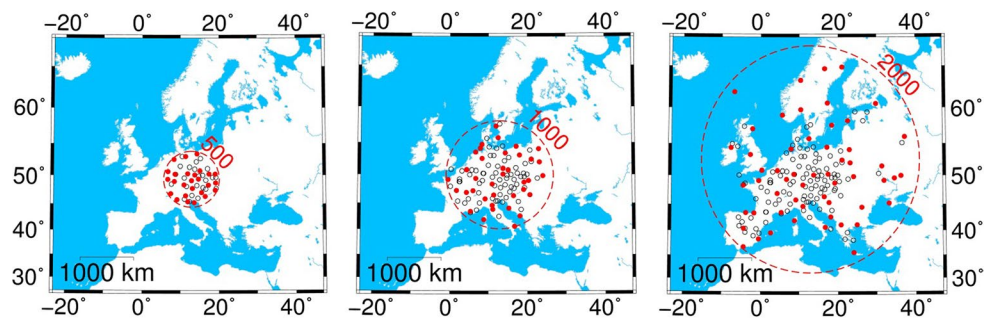
Fig. 1 Different scale of GPS/GLONASS networks in Europe from the EUREF and IGS. Red solid circles denote stations used for the FCB estimation. Black open circles denote stations used to test PPP-AR. Shown in panel left, middle and right are the small, medium and large networks, covering circular areas with radii of 500, 1000 and 2000 km centered at station WTZR, respectively

Table 1 Number of stations for each receiver family

Receiver family	Number of station
Javad	3
JPS	22
Leica	81
NovAtel	4
Septentrio Polarx	5
TPS	13
Trimble	37

resolution. The precisions of pseudorange and carrier phase measurements were presumed to be 2 m and 2 cm, respectively. The phase center offset and variation corrections were also applied (Dach et al. 2011; Schmid et al. 2007). The phase wind-up effects were corrected (Wu et al. 1993). The mapping function of zenith troposphere delays was VMF1 (Vienna Mapping Function 1) (Boehm et al. 2006), and the power spectral density for zenith wet components was set as 2 cm/$\sqrt{h}$. The receiver position, the receiver clocks, the zenith tropospheric delays and horizontal gradients and the ambiguities were estimated. FCBs were re-estimated every 15 min, and no constraints on neighboring FCB estimates were applied. Rejection of outlier ambiguity fractional parts for the FCB estimation was carried out using a threshold of three times the standard deviation and the sign-constrained robust least squares method (Xu 2005). Based on the method proposed by Liu et al. (2016), the receiver carrier phase IFBs were estimated with respect to the values listed by Wanninger (2012). The LAMBDA (Teunissen 1995; De Jonge and Tiberius 1996) method was used to search for integer ambiguities, and the ratio test, which is defined as the ratio between the weighted sum of the squared residuals of the second best solution to that of the best, was used to validate integer candidates. The threshold of the ratio test was 3.0 throughout in this study.

In order to investigate how the network extent affects the performance of ionospheric-free FCB estimation and PPP-AR, we tried three scales of networks which cover circular areas with radii of 500, 1000 and 2000 km centered at station WTZR. In the following, they are denoted as the small, medium and large networks including 52, 107 and 165 stations, respectively. Within each network, we chose a few tens of stations, i.e., 26, 37 and 55, respectively, to estimate FCBs whereas the remaining stations were used to test PPP-AR. For each network, we computed three types of solutions:

- "GLONASS-only and GLONASS fixed" solutions where only GLONASS data were processed, and only GLONASS ionospheric-free ambiguity fixing was attempted;
- "GLONASS + GPS and GLONASS fixed" solutions where both GLONASS and GPS data were processed, but only GLONASS ionospheric-free ambiguities were fixed;
- "GLONASS + GPS and both fixed" where both GLONASS and GPS data were processed, and all relevant ambiguities were fixed. Note that wide-lane and narrow-lane ambiguities were fixed for GPS.

In addition, for each type of solutions, we also tried different observation durations, i.e., 1, 2 and 3 h. Then the efficiency of GLONASS ionospheric-free ambiguity resolution and the positioning performance with respect to the observation durations are presented and discussed. Float solutions which are eligible for PPP-AR are defined as those that have five and more undifferenced GLONASS ambiguities to be resolved. If five or more GLONASS ambiguities are resolved and the positioning differences for the truth benchmark in the east and north components are both below 2 cm, this solution will be considered as a correctly fixed solution. In this study, daily solutions are taken as the truth benchmarks. The ambiguity fixing rate is

defined as the percentage of resolved ambiguity within all eligible ones. The correctly fixed ambiguity rate is defined as the percentage of correctly fixed ambiguities within all fixed ambiguities. Here, the daily ambiguity estimates were used as the reference values.

Results

In this section, we will first analyze the performance of GLONASS FCB estimation and then, inspect the efficiency of GLONASS ionospheric-free ambiguity resolution and the positioning performance, and finally, the contribution of ambiguity-fixed GLONASS orbits to GLONASS PPP-AR is investigated.

GLONASS ionospheric-free FCB estimation

The ionospheric-free FCB estimates on day 300 for eight exemplary satellites and the distribution of relevant fractional parts after removal of FCBs for all GLONASS satellites over consecutive 31 days are shown in Fig. 2. We note that the FCBs are estimated using only the reference stations within each network, while the distribution of fractional parts in Fig. 2 is based on the solutions from all stations. It can be seen that the ionospheric-free FCB time series change very smoothly and steadily over time. The FCBs for R12 from 11 to 14 h derived from the large network show drastic jumps of up to 0.5 cycles, which is marked with a dashed square. We contend that these jumps are due to the low elevation (< 20°) of R12 during the entire observation periods with respect to all stations, which leads to noisy ambiguity estimates. Overall, the ionospheric-free FCB estimates from all networks vary minimally within a continuous observation period.

The distribution of the fractional parts after removal of FCBs is an important diagnostics to assessing the quality of FCB estimations. The closer to zero such a fractional part is, the more accurate FCBs we have estimated and the more reliable PPP-AR can be achieved potentially. For the small network, 89.9% of all fractional parts fall in the range
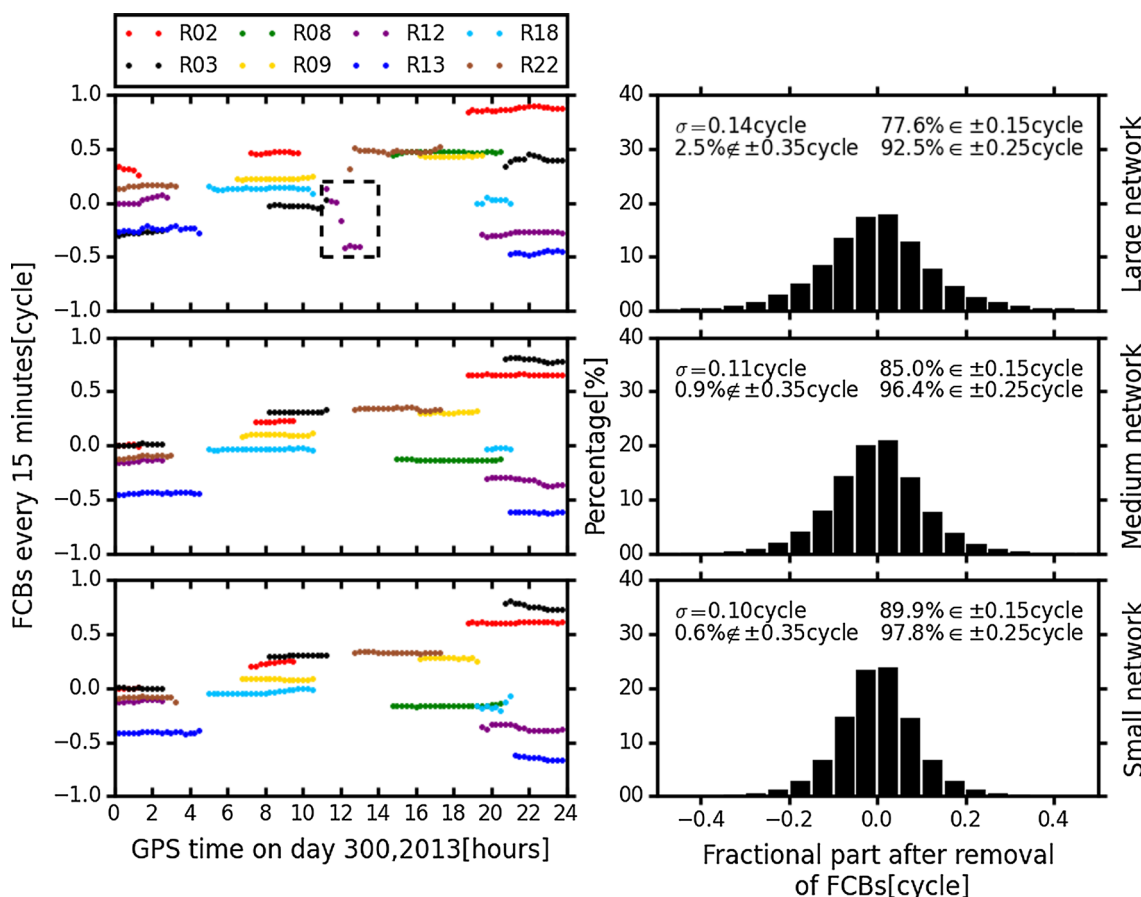
Fig. 2 GLONASS ionospheric-free FCBs for eight satellites estimated every 15 min over reference stations on day 300 of 2013 (left column) and distribution of all fractional parts after removal of FCBs over the 31 days (right column), for large (top), medium (middle) and small network (bottom). σ denotes the standard deviation of the fractional parts. $\in$ means 'within' while $\notin$ means 'outside'

of ± 0.15 cycles, 97.8% in ± 0.25 cycles and 0.6% outside ± 0.35 cycles with a standard deviation of 0.10 cycles. Comparatively, the medium network performs slightly worse, with 85.0% falling in ± 0.15 cycles and a standard deviation of 0.11 cycles. As the network size is increased, the performance of FCB estimation is worsened. In particular, for the large network, there are only 77.6% of fractional parts falling in ± 0.15 cycles. This phenomenon can be understood in terms of the fact that the larger the network is, the error correlation among stations gets weaker. As a result, the spatially correlated errors, such as orbits and atmosphere refractions, cannot be absorbed into the FCB estimates, resulting in poor agreement among the fractional parts of ionospheric-free ambiguities from all involved stations. Although Fig. 2 shows that GLONASS ionospheric-free FCBs have excellent temporal stability and the fractional parts are overall in good agreement, their performance is still worse than those for the GLONASS narrow-lane FCBs in Geng and Bock (2016). Even for the small network, for example, 89.9% of all fractional parts were located in the range of ± 0.15 cycles, which is below the 99% reported by them. This should be caused by the shorter wavelength of ionospheric-free ambiguities than that of narrow-lane ambiguities.

GLONASS-only PPP-AR

Stations involved in static PPP of this study are exclusive of reference stations, which are used to estimate FCBs above. Table 2 shows GLONASS-only static PPP solutions. PPP-AR improves the positioning accuracy significantly, since the RMS for the east, north and up components with respect to the daily position estimates for the small network is reduced from 1.5, 1.0, 2.3 cm for the float solutions to 0.6, 0.5, 1.9 cm for the fixed solutions, which equates an improvement of 60, 50 and 17%, respectively. Such improvement can also be clearly found for the medium and large networks, where the east component is improved most. When the observation period is increased from 1 to 2 and 3 h, the positioning accuracy of float solutions steadily improves (Table 2), and ionospheric-free ambiguity fixing still contributes significantly to the improvement in positioning accuracy, which agrees with Banville (2016).

In the case of hourly data, the percentages of fixed solutions and fixed ambiguities are only 66.8 and 74.4%, respectively, for a small network, which is obviously worse than that of GPS (Geng et al. 2010b). When the observation period is increased to 2 and 3 h, the percentage of correctly fixed solutions increases to 90.1 and 97.5%, respectively, while the percentage of fixed ambiguities increases to 91.7 and 97.6%, respectively. This is expected as longer observation periods should lead to higher accuracy of ambiguity estimates, which in turn improve the efficiency of ambiguity fixing. Furthermore, even for 1 h observation periods, the percentage of correctly fixed ambiguities can achieve 94.8 and 98.5% for 3 h, suggesting that this percentage is slightly affected by the length of observation periods. This indicates that once the GLONASS ionospheric-free ambiguities are presumably resolved after the LAMBDA search and the ratio test, they can normally be fixed to the correct integers, even for 1 h observation

Table 2 Results of hourly static PPP with GLONASS-only data from rover stations over the 31 days

Scale of network	Fixed sol. [%]	East [cm] fixed/float	North [cm] fixed/float	Up [cm] fixed/float	Fixed amb. [%]	Correct amb. [%]
1 hourly						
Small	66.8	0.6/1.5	0.5/1.0	1.9/2.3	74.4	94.8
Medium	63.4	0.6/1.5	0.6/1.0	1.9/2.3	71.8	94.0
Large	61.7	0.7/1.5	0.6/1.0	2.1/2.3	70.9	93.3
2 hourly						
Small	90.1	0.4/1.3	0.4/0.7	1.2/1.5	91.7	98.7
Medium	87.8	0.5/1.3	0.4/0.7	1.3/1.5	89.9	98.5
Large	84.4	0.5/1.2	0.5/0.7	1.5/1.6	86.8	98.1
3 hourly						
Small	97.5	0.4/1.0	0.4/0.6	1.1/1.2	97.6	98.5
Medium	97.5	0.4/1.0	0.4/0.6	1.2/1.3	97.1	98.5
Large	95.8	0.5/1.0	0.4/0.6	1.3/1.4	94.8	98.2

Column "Fixed sol." shows the percentage of correctly fixed solutions among all solutions to be fixed. In columns "East", "North", "Up" are the RMS (cm) of fixed and float hourly solutions with respect to daily solutions, separated by "/". Column "Fixed amb." shows the percentage of resolved ambiguities within all eligible ones. Column "Correct amb." shows the percentage of correctly fixed ambiguities within all fixed ones, and the criterion of the correct ambiguities is the equivalence between the hourly and the daily ambiguity estimates

periods. Moreover, Table 2 shows that when the observation periods reach 3 h, a fairly reliable AR can be achieved for GLONASS-only static PPP. For example, the percentages of the fixed solutions and the fixed ambiguities can reach 95.8 and 94.8% for the large network, respectively.

Integrated GLONASS and GPS PPP-AR

Table 3 shows static PPP results for "GLONASS + GPS and GLONASS fixed" solutions and "GLONASS + GPS and both fixed" solutions. Taking the small network as an example, the percentage of correctly fixed solution increases from 66.8 to 80.6%, and the percentage of fixed GLONASS ambiguities also increases from 74.4 to 83.8% in case of 1 h observation periods, after introducing GPS data into GLONASS solutions while only GLONASS ambiguities are fixed. Meanwhile, the RMS for the east, north and up components with respect to daily solutions is decreased from 0.6, 0.5, 1.9 cm to 0.5, 0.5, 1.3 cm, respectively. If GPS PPP-AR is further performed, the percentage of correctly fixed solution can be improved from 80.6 to 95.9% and the percentage of fixed GLONASS ambiguities also improves from 83.8 to 95.4%. The RMS for the east, north and up components is reduced further to 0.4, 0.4, 1.1 cm, respectively.

When the length of observation period is increased from 1 to 2 and 3 h, the percentage of correctly fixed solutions increases from 80.6 to 95.6 and 99.4%, respectively, in case of the "GLONASS + GPS and GLONASS fixed" solutions. In contrast, the percentage of correctly fixed solutions increases from 95.9 to 99.0 and 99.4%, respectively, in case of the "GLONASS + GPS and both fixed" solutions. From Table 3, we can see that the performance of the "GLONASS + GPS and both fixed" solutions in case of 2 h observation periods is at the similar level to those of the "GLONASS-only and GLONASS fixed" and "GLONASS + GPS and GLONASS fixed" solutions in case of 3 h observation periods. In general, introducing GPS data and subsequently fixing GPS ambiguities can improve the positioning performance significantly, especially the success rate of GLONASS ambiguity resolution.

GLONASS PPP-AR in case of ambiguity-fixed GLONASS orbits

GLONASS orbit errors are one of the major factors that affect the performance of PPP-AR, especially in case of a large network. The orbit accuracy can be significantly improved after successful ambiguity resolution over the reference network

Table 3 Results of hourly static PPP at rover stations over the 31 days

Type of solution	Scale of network	Fixed sol.[%]	East [cm]	North [cm]	Up [cm]	Fixed amb. [%]
1 hourly						
GLONASS + GPS and GLONASS fixed	Small	80.6	0.5/1.3	0.5/0.8	1.3/1.6	83.8
	Medium	75.0	0.6/1.3	0.5/0.8	1.4/1.6	79.4
	Large	72.1	0.6/1.3	0.6/0.8	1.6/1.7	77.4
GLONASS + GPS and both fixed	Small	95.9	0.4/1.8	0.4/1.0	1.1/1.8	95.4
	Medium	93.1	0.4/1.8	0.5/1.0	1.2/1.9	92.8
	Large	90.9	0.5/1.8	0.5/1.0	1.4/1.9	89.8
2 hourly						
GLONASS + GPS and GLONASS fixed	Small	95.6	0.4/1.0	0.4/0.6	1.0/1.1	96.3
	Medium	93.1	0.5/1.0	0.5/0.6	1.0/1.2	94.0
	Large	91.0	0.5/1.0	0.5/0.6	1.2/1.3	91.7
GLONASS + GPS and both fixed	Small	99.0	0.4/1.1	0.4/0.6	0.9/1.2	98.4
	Medium	98.0	0.4/1.1	0.4/0.6	1.0/1.2	96.8
	Large	96.7	0.4/1.1	0.5/0.6	1.1/1.3	94.4
3 hourly						
GLONASS + GPS and GLONASS fixed	Small	99.4	0.4/0.7	0.4/0.5	0.83/0.94	98.8
	Medium	98.8	0.4/0.8	0.4/0.5	0.93/1.01	97.7
	Large	97.8	0.5/0.8	0.4/0.5	1.04/1.09	95.7
GLONASS + GPS and both fixed	Small	99.4	0.3/0.7	0.4/0.5	0.78/0.95	98.1
	Medium	98.1	0.4/0.8	0.4/0.5	0.86/1.01	95.7
	Large	95.9	0.4/0.8	0.4/0.5	0.97/1.09	91.7

Column "Fixed sol." shows the percentage of correctly fixed solutions among all those to be fixed. In columns "East", "North", "Up" are the RMS (cm) of fixed and float solutions with respect to daily solutions, separated by "/". Column "Fixed amb." shows the percentage of resolved GLONASS ambiguities within all eligible GLONASS ones

used for orbit determination. In this section, we will use both ambiguity-fixed and ambiguity-float orbits to investigate the performance of GLONASS PPP-AR. At present, the GLONASS products of IGS analysis centers are mainly based on the float ambiguities, except for those from CODE (Centre for Orbit Determination in Europe). The ambiguity-fixed orbit product used in this section is derived using the method by Liu et al. (2016). We re-computed the "GLONASS-only and GLONASS fixed" solutions with the large network for day 300–330 in 2013.

The results are shown in Fig. 3 and Table 4. Compared to the results from float orbits, the results of fixed orbits have a better performance, and the percentages of the fractional parts within ± 0.15 cycles increase substantially from 74.6 to 80.5%, those within ± 0.25 cycles increase from 90.4 to 94.0% and those outside ± 0.35 cycles decrease from 3.6 to 2.0% on average. In particular, the percentages of the fractional parts within range ± 0.15 cycle vary from 72.2 to 85.4% for the fixed orbits, in contrast to 59.4–82.8% for the float orbits, which shows that

the performance with respect to the fixed orbits is better. The percentages of the correctly fixed solution with respect to the fixed orbits are 63.1%, but just 60.2% with respect to the float orbits in case of 1 h observation periods. The percentages of fixed ambiguities within all candidate ambiguities are 71.4 and 68.6% for fixed and float orbits, respectively. Compared to the float orbits, the performance of static PPP-AR for the fixed orbits improves in terms of the fixing rate of ambiguities and the positioning accuracy. Therefore, for a large network spanning over a few 1000 km, ambiguity-fixed GLONASS orbit will clearly benefit GLONASS PPP-AR.

Conclusions

This study investigates GLONASS PPP-AR based on the ionospheric-free ambiguities with a wavelength of about 5.3 cm, motivated by Banville (2016) and Liu et al. (2016).

Fig. 3 Distribution of all fractional parts after removal of FCBs over the 31 days. σ denotes the standard deviation of the fractional parts. $\in$ means 'within' while $\notin$ means 'outside'. Red and black represent ambiguity-fixed and- float orbits
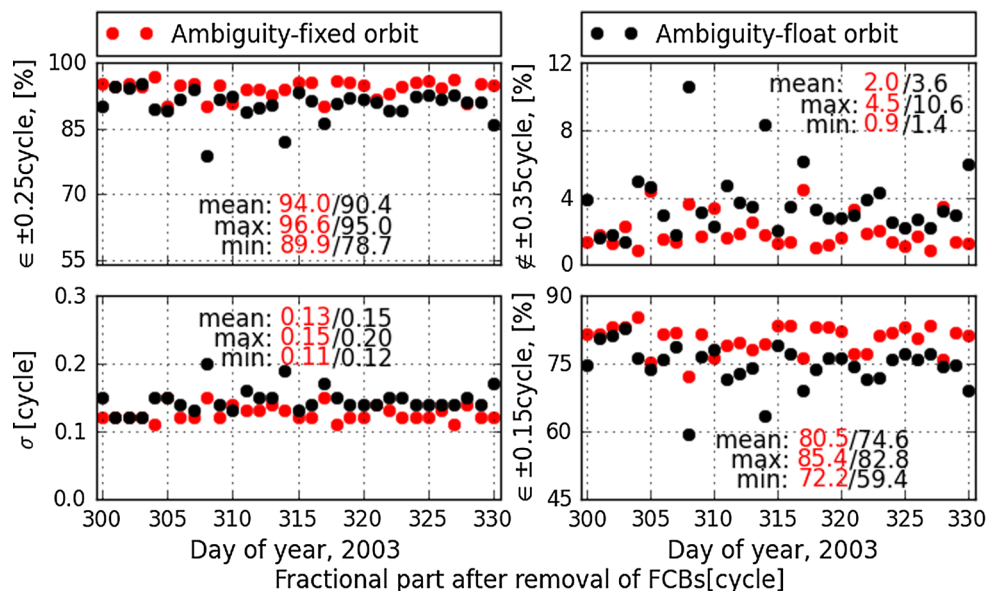
Table 4 Results of hourly static PPP of the ambiguity-fixed and-float orbits from rover stations within large network over the 31 days

Time	Fixed sol. [%]	East [cm]	North [cm]	Up [cm]	Fixed amb. [%]
Ambiguity-fixed orbit					
1 hourly	63.1	0.62/1.45	0.59/1.01	1.91/2.22	71.4
2 hourly	86.6	0.49/1.23	0.48/0.72	1.36/1.52	88.4
3 hourly	96.3	0.47/0.98	0.44/0.58	1.17/1.21	95.5
Ambiguity-float orbit					
1 hourly	60.2	0.66/1.43	0.63/1.01	1.98/2.20	68.6
2 hourly	82.7	0.52/1.20	0.51/0.72	1.40/1.50	85.1
3 hourly	94.4	0.50/0.95	0.46/0.59	1.19/1.20	93.4

Column "Fixed sol." shows the percentage of correctly fixed solutions within all those to be fixed. In columns "East", "North", "Up" are the RMS (cm) of fixed and float hourly solutions with respect to daily solutions, separated by "/". Column "Fixed amb." shows the percentage of resolved GLONASS ambiguities within all candidate GLONASS ones

The data processing strategy is fairly straightforward as pseudorange IFBs are no longer a factor in deterring PPP-AR. With the data from day 300–331 in 2013 from about 165 stations in Europe, the performance of GLONASS PPP-AR is investigated with different network sizes, types of solution and lengths of the observation period.

The distribution of the fractional parts after removal of FCBs is an important diagnostics to assessing the quality of FCB estimations. For the small network, we find that 89.9% of all fractional parts agree well within ± 0.15 cycles with a standard deviation of 0.10 cycles. The performance slightly decreases when the size of the network increases, and 77.6% of fractional parts are within ± 0.15 cycle with a standard deviation of 0.14 cycle for the large network.

When the length of observation period reaches 3 h, a fairly reliable PPP-AR can be achieved for GLONASS-only static PPP. The percentages of fixed solution and fixed ambiguities can reach 97.5 and 97.6%, respectively, for the small network. The RMS of east, north and up directions decreases from 1.0, 0.6, 1.2 cm to 0.4, 0.4, 1.1 cm by 60.0, 33.3 and 8.3%, respectively.

Introducing GPS and simultaneously fixing GPS ambiguities, the performance of positioning is improved to a large extent, especially increasing the percentages of fixed GLONASS ambiguities. For the solution type "GLONASS + GPS and both fixed," the small network and the 1-h observation period, compared to solution type "GLONASS-only and GLONASS fixed" the percentage of fixed GLONASS ambiguity increases from 74.4 to 95.4%. For the 2-h observation period, the percentage of fixed ambiguity can reach 98.4% for the small network and also can reach 94.4% for the large network. The performance of static PPP-AR shows higher efficiency and reliability than the solution type "GLONASS-only and GLONASS fixed" of the 3-h observation period. Overall, we demonstrate that 2 h of data can usually ensure a reliable GLONASS PPP-AR which is comparable to what can be obtained with 3 h of data.

Ambiguity-fixed and- float orbits are used to evaluate the effect of orbital errors on the performance of PPP-AR. The results show that for the large network, the fractional parts of ambiguity-fixed orbits have better consistency and show more stability from day to day than from ambiguity-float orbits. The percentages of GLONASS fixed ambiguities are 71.4 and 68.6% for ambiguity-fixed and ambiguity-float orbits for the 1-h observation period, respectively. A GLONASS ambiguity-fixed orbit is necessary, which makes AR more effective. Generally, a high precision orbit can effectively improve the performance of PPP-AR over a large network.

References

Al-Shaery A, Zhang S, Rizos C (2013) An enhanced calibration method of GLONASS inter-channel bias for GNSS RTK. GPS Solut 17(2):165–173

Banville S (2016) GLONASS ionosphere-free ambiguity resolution for precise point positioning. J Geod 90(5):487–496

Bertiger W, Desai SD, Haines B, Harvey N, Moore AW, Owen S, Weiss JP (2010) Single receiver phase ambiguity resolution with GPS data. J Geod 84(5):327–337

Boehm J, Werl B, Schuh H (2006) Troposphere mapping functions for GPS and very long baseline interferometry from European Centre for Medium-Range Weather Forecasts operational analysis data. J Geophys Res. https://doi.org/10.1029/2005JB003629

Cheng S, Wang J, Peng W (2017) Statistical analysis and quality control for GPS fractional cycle bias and integer recovery clock estimation with raw and combined observation models. Adv Space Res. https://doi.org/10.1016/j.asr.2017.06.053

Collins P, Bisnath S, Lahaye F, Héroux P (2010) Undifferenced GPS ambiguity resolution using the decoupled clock model and ambiguity datum fixing. Navigation 57(2):123–135

Dach R, Schmid R, Schmitz M, Thaller D, Schaer S, Lutz S, Steigenberger P, Wubbena G, Beutler G (2011) Improved antenna phase center models for GLONASS. GPS Solut 15(1):49–65

Dai L (2000) Dual-frequency GPSGLONASS real-time ambiguity resolution for medium-range kinematic positioning. In: ION GPS 2000, 19–22 Sept 2000, Salt Lake City, pp 1071–1080

De Jonge P, Tiberius C (1996) The LAMBDA method for integer ambiguity estimation: implementation aspects. Publications of the Delft Computing Centre, LGR-Series 12

Ge M, Gendt G, Rothacher M, Shi C, Liu J (2008) Resolution of GPS carrier-phase ambiguities in precise point positioning (PPP) with daily observations. J Geod 82(7):389–399

Geng J, Bock Y (2016) GLONASS fractional-cycle bias estimation across inhomogeneous receivers for PPP ambiguity resolution. J Geod 90(4):379–396

Geng J, Shi C (2017) Rapid initialization of real-time PPP by resolving undifferenced GPS and GLONASS ambiguities simultaneously. J Geod 91(4):361–374

Geng J, Meng X, Dodson A, Teferle F (2010a) Integer ambiguity resolution in precise point positioning: method comparison. J Geod 84(9):569–581

Geng J, Meng X, Teferle FN, Dodson AH (2010b) Performance of precise point positioning with ambiguity resolution for 1- to 4-h observation periods. Surv Rev 42(316):155–165

Geng J, Shi C, Ge M, Dodson AH, Lou Y, Zhao Q, Liu J (2012) Improving the estimation of fractional-cycle biases for ambiguity resolution in precise point positioning. J Geod 86(8):579–589

Geng J, Zhao Q, Shi C, Liu J (2017) A review on the inter-frequency biases of GLONASS carrier-phase data. J Geod 91(3):329–340

Hatch R (1982) The synergism of GPS code and carrier measurements. In: Proceedings of the third international symposium on satellite Doppler positioning at Physical Sciences Laboratory of New Mexico State University, vol 2, 8–12 Feb, pp 1213–1231

Laurichesse D, Mercier F, Berthias JP, Broca P, Cerri L (2009) Integer ambiguity resolution on undifferenced GPS phase measurements and its application to PPP and satellite precise orbit determination. Navigation 56(2):135–149

Leick A, Beser J, Li J, Mader G (1995) Processing GLONASS carrier phase observations-theory and first experience. In: Proceedings of ION-GPS-95, Institute of Navigation, Palm Springs, California, pp 1041–1047

Liu Y, Ge MR, Shi C, Lou YD, Wickert J, Schuh H (2016) Improving integer ambiguity resolution for GLONASS precise orbit determination. J Geod 90(8):715–726

Reussner N, Wanninger L (2011) GLONASS inter-frequency biases and their effects on RTK and PPP carrier phase ambiguity resolution. In: Proceedings ION GNSS 2011, Institute of Navigation, Portland, OR, pp 712–716

Roßbach U (2000) Positioning and navigation using the Russian satellite system GLONASS. Ph.D. Thesis, Universitaet der Bundeswehr Muenchen

Schmid R, Steigenberger P, Gendt G, Ge M, Rothacher M (2007) Generation of a consistent absolute phase-center correction model for GPS receiver and satellite antennas. J Geod 81(12):781–798

Shi C, Yi W, Song W, Lou Y, Yao Y, Zhang R (2013) GLONASS pseudorange inter-channel biases and their effects on combined GPS/GLONASS precise point positioning. GPS Solut 17(4):439–451

Sleewaegen JM, Simsky A, De Wilde W, Boon F, Willems T (2012) Demystifying GLONASS inter-frequency carrier phase biases. Inside GNSS 7(3):57–61

Teunissen PJG (1995) The least-squares ambiguity decorrelation adjustment: a method for fast GPS integer ambiguity estimation. J Geod 70(1):65–82

Wang J (2000) An approach to GLONASS ambiguity resolution. J Geod 74(5):421–430

Wang J, Rizos C, Stewart MP, Leick A (2001) GPS and GLONASS integration: modeling and ambiguity resolution issues. GPS Solut 5(1):55–64

Wanninger L (2012) Carrier-phase inter-frequency biases of GLONASS receivers. J Geod 86(2):139–148

Wu JT, Wu SC, Hajj GA, Bertiger WI, Lichten SM (1993) Effects of antenna orientation on GPS carrier phase. Manuscr Geodaet 18(2):91–98

Xu P (2005) Sign-constrained robust least squares, subjective breakdown point and the effect of weights of observations on robustness. J Geod 79(1–3):146–159

Yamada H, Takasu T, Kubo N, Yasuda A (2010) Evaluation and calibration of receiver inter-channel biases for RTK-GPS/GLONASS. In: Proceedings of the 23rd international technical meeting of The Satellite Division of the Institute of Navigation, Portland, OR, pp 1580–1587

Qile Zhao is a professor of GNSS Research Center of Wuhan University. He received his Ph.D. degree in Wuhan University in 2004. In 2006–2007, as a postdoctoral fellow, he did his postdoctoral program in DEOS, Delft University of Technology, the Netherlands. His current research interests are precise orbit determination of GNSS and low earth orbit satellites, and high-precision positioning using GNSS.

Xiaotao Li is currently a Ph.D. candidate at GNSS Research Center, Wuhan University. He received his bachelor degree in 2011 from Chang'an University. His current research mainly focuses on high-precision positioning using GNSS.

Yang Liu is currently a postdoctoral researcher at Wuhan University. He received his bachelor degree in geomatics engineering from School of Geodesy and Geomatics, Wuhan University, in 2010. He received his Ph.D. degree in geodesy and surveying engineering from GNSS Research Center, Wuhan University, in 2016. His main research interests include real-time precise orbit determination of GNSS and LEO satellites and geophysical applications.

Jianghui Geng has been a professor in GNSS geodesy at Wuhan University since 2015. He graduated from the University of Nottingham in the UK in 2011. Afterward, he had an enterprise fellowship from the Nottingham Geospatial Institute in 2011 and a Green scholarship from Scripps Institution of Oceanography from 2012 to 2014. He was promoted as an assistant project scientist in 2015 (see homepage: pride.whu. edu.cn). His major research interest is high-precision GNSS.

Jingnan Liu graduated from the former Wuhan College of Surveying and Mapping in 1967 and received his master's degree in 1982. He was elected Academician of the Chinese Academy of Engineering in 1999. He has been a member of the Science and Technology Committee, Ministry of Education of China, in 1997–2009 and as an editorial board member of GPS Solutions in 1998–2000. He is currently an executive member of the council, Chinese Society for Geodesy Photogrammetry and Cartography; the editorial board member of GPS World; and the coordinator of International GPS Geodynamics Services. His current research interests are satellite precise orbit determination.